

Basis Functions for Linear-Scaling First-Principles Calculations

E. Hernández and M. J. Gillan

Physics Department, Keele University, Staffordshire ST5 5BG, U.K.

C. M. Goringe

Materials Department, Oxford University, Oxford OX1 3PH, U.K.

(October 28, 2018)

In the framework of a recently reported linear-scaling method for density-functional-pseudopotential calculations, we investigate the use of localized basis functions for such work. We propose a basis set in which each local orbital is represented in terms of an array of “blip functions” on the points of a grid. We analyze the relation between blip-function basis sets and the plane-wave basis used in standard pseudopotential methods, derive criteria for the approximate equivalence of the two, and describe practical tests of these criteria. Techniques are presented for using blip-function basis sets in linear-scaling calculations, and numerical tests of these techniques are reported for Si crystal using both local and non-local pseudopotentials. We find rapid convergence of the total energy to the values given by standard plane-wave calculations as the radius of the linear-scaling localized orbitals is increased.

arXiv:mtrl-th/9609003v1 20 Sep 1996

I. INTRODUCTION

First-principles calculations based on density functional theory^{1,2} (DFT) and the pseudopotential method are widely used for studying the energetics, structure and dynamics of solids and liquids³⁻⁵. In the standard approach, the occupied Kohn-Sham orbitals are expanded in terms of plane waves, and the ground state is found by minimizing the total energy with respect to the plane-wave coefficients⁶. Calculations on systems of over a hundred atoms with this approach are now quite common. However, it has proved difficult to go to very much larger systems, because the computational effort in this approach depends on the number of atoms N at least as N^2 , and asymptotically as N^3 . Because of this limitation, there has been a vigorous effort in the past few years to develop linear-scaling methods⁷⁻²⁴ – methods in which the effort depends only linearly on the number of atoms. We have recently described a general theoretical framework for developing linear-scaling self-consistent DFT schemes^{22,23}. We presented one practical way of implementing such a scheme, and investigated its performance for crystalline silicon. Closely related ideas have been reported by other authors^{21,24} – an overview of work on linear-scaling methods was given in the Introduction of our previous paper²³.

The practical feasibility of linear-scaling DFT techniques is thus well established. However, there are still technical problems to be solved before the techniques can be routinely applied. Our aim here is to study the problem of representing the localized orbitals that appear in linear-scaling methods (support functions in our terminology) – in other words, the problem of basis functions. To put this in context, we recall briefly the main ideas of our linear-scaling DFT method.

Standard DFT can be expressed in terms of the Kohn-Sham density matrix $\rho(\mathbf{r}, \mathbf{r}')$. The total-energy functional can be written in terms of ρ , and the ground state is obtained by minimization with respect to ρ subject to two constraints: ρ is idempotent (it is a projector, so that its eigenvalues are 0 or 1), and its trace is equal to half the number of electrons. Linear-scaling behavior is obtained by imposing a limitation on the spatial range of ρ :

$$\rho(\mathbf{r}, \mathbf{r}') = 0, \quad |\mathbf{r} - \mathbf{r}'| > R_c. \quad (1)$$

By the variational principle, we then get an upper bound $E(R_c)$ to the true ground-state energy E_0 . Since the true ground-state density matrix decays to zero as $|\mathbf{r} - \mathbf{r}'| \rightarrow \infty$, we expect that $E(R_c \rightarrow \infty) = E_0$. To make the scheme practicable, we introduced the further condition that ρ be separable:

$$\rho(\mathbf{r}, \mathbf{r}') = \sum_{\alpha\beta} \phi_\alpha(\mathbf{r}) K_{\alpha\beta} \phi_\beta(\mathbf{r}'), \quad (2)$$

where the number of support functions $\phi_\alpha(\mathbf{r})$ is finite. The limitation on the spatial range of ρ is imposed by

requiring that the $\phi_\alpha(\mathbf{r})$ are non-zero only in localized regions (“support regions”) and that the spatial range of $K_{\alpha\beta}$ is limited. In our method, the support regions are centered on the atoms and move with them.

We have shown^{22,23} that the condition on the eigenvalues of ρ can be satisfied by the method of Li, Nunes and Vanderbilt¹⁹ (LNV): instead of directly varying ρ , we express it as:

$$\rho = 3\sigma * \sigma - 2\sigma * \sigma * \sigma, \quad (3)$$

where the asterisk indicates the continuum analog of matrix multiplication. As shown by LNV, this representation of ρ not only ensures that its eigenvalues lie in the range $[0, 1]$, but it drives them towards the values 0 and 1. In our scheme, the auxiliary matrix $\sigma(\mathbf{r}, \mathbf{r}')$ has the same type of separability as ρ :

$$\sigma(\mathbf{r}, \mathbf{r}') = \sum_{\alpha\beta} \phi_\alpha(\mathbf{r}) L_{\alpha\beta} \phi_\beta(\mathbf{r}'). \quad (4)$$

This means that K is given by the matrix equation:

$$K = 3LSL - 2LSLSL, \quad (5)$$

where $S_{\alpha\beta}$ is the overlap matrix of support functions:

$$S_{\alpha\beta} = \int d\mathbf{r} \phi_\alpha \phi_\beta. \quad (6)$$

We can therefore summarize the overall scheme as follows. The total energy is expressed in terms of ρ , which depends on the separable quantity σ . The ground-state energy is obtained by minimization with respect to the support functions $\phi_\alpha(\mathbf{r})$ and the matrix elements $L_{\alpha\beta}$, with the ϕ_α confined to localized regions centered on the atoms, and the $L_{\alpha\beta}$ subject to a spatial cut-off.

The $\phi_\alpha(\mathbf{r})$ must be allowed to vary freely in the minimization process, just like the Kohn-Sham orbitals in conventional DFT, and we must consider how to represent them. As always, there is a choice: we can represent them either by their values on a grid²⁵⁻³⁴, or in terms of some set of basis functions. In our previous work^{22,23}, we used a grid representation. This was satisfactory for discussing the feasibility of linear-scaling schemes, but seems to us to suffer from significant drawbacks. Since the support regions are centered on the ions in our method, this means that when the ions move, the boundaries of the regions will cross the grid points. In any simple grid-based scheme, this will cause troublesome discontinuities. In addition, the finite-difference representation of the kinetic-energy operator in a grid representation causes problems at the boundaries of the regions. A further point is that in a purely grid-based method we are almost certainly using more variables than are really necessary. These problems have led us to consider basis-function methods.

We describe in this paper a practical basis-function scheme for linear-scaling DFT, and we study its performance in numerical calculations. The basis consists of

an array of localized functions – we call them “blip functions”. There is an array of blip functions for each support region, and the array moves with the region. The use of such arrays of localized functions as a basis for quantum calculations is not new^{35–38}. However, to our knowledge it has not been discussed before in the context of linear-scaling calculations.

The plan of the paper is as follows. In Sec. 2, we emphasize the importance of considering the relation between blip-function and plane-wave basis sets, and we use this relation to analyze how the calculated ground-state energy will depend on the width and spacing of the blip functions. We note some advantages of using B-splines as blip functions, and we then present some practical tests which illustrate the convergence of the ground-state energy with respect to blip width and spacing. We then go on (Sec. 3) to discuss the technical problems of using blip-function basis sets in linear-scaling DFT. We report the results of practical tests, which show explicitly how the ground-state energy in linear-scaling DFT converges to the value obtained in a standard plane-wave calculation. Section 4 gives a discussion of the results, and presents our conclusions. Some mathematical derivations are given in an appendix.

II. BLIP FUNCTIONS AND PLANE WAVES

A. General considerations

Before we focus on linear-scaling problems, we need to set down some elementary ideas about basis functions. To start with, we therefore ignore the linear-scaling aspects, and we discuss the general problem of solving Schrödinger’s equation using basis functions. It is enough to discuss this in one dimension, and we assume a periodically repeating system, so that the potential $V(x)$ acting on the electrons is periodic: $V(x+t) = V(x)$, where t is any translation vector. Self-consistency questions are irrelevant at this stage, so that $V(x)$ is given. The generalization to three-dimensional self-consistent calculations will be straightforward.

In a plane-wave basis, the wavefunctions $\psi_i(x)$ are expanded as

$$\psi_i(x) = L^{-1/2} \sum_G c_{iG} \exp(iGx), \quad (7)$$

where the reciprocal lattice vectors of the repeating geometry are given by $G = 2\pi n/L$ (n is an integer), and we include all G up to some cut-off G_{\max} . We obtain the ground-state energy $E(G_{\max})$ in the given basis by minimization with respect to the c_{iG} , subject to the constraints of orthonormality. For the usual variational reasons, $E(G_{\max})$ is a monotonically decreasing function of G_{\max} which tends to the exact value E_0 as $G_{\max} \rightarrow \infty$.

Now instead of plane waves we want to use an array of spatially localized basis functions (blip functions). Let

$f_0(x)$ be some localized function, and denote by $f_\ell(x)$ the translated function $f_0(x-\ell a)$, where ℓ is an integer and a is a spacing, which is chosen so that L is an exact multiple of a : $L = Ma$. We use the array of blip functions $f_\ell(x)$ as a basis. Equivalently, we can use any independent linear combinations of the $f_\ell(x)$. In considering the relation between blip functions and plane waves, it is particularly convenient to work with “blip waves”, $\chi_G(x)$, defined as:

$$\chi_G(x) = A_G \sum_{\ell=0}^{M-1} f_\ell(x) \exp(iGR_\ell), \quad (8)$$

where $R_\ell = \ell a$, and A_G is some normalization constant.

The relation between blip waves and plane waves can be analyzed by considering the Fourier representation of $\chi_G(x)$. It is straightforward to show that $\chi_G(x)$ has Fourier components only at wavevectors $G + \Gamma$, where Γ is a reciprocal lattice vector of the blip grid: $\Gamma = 2\pi m/a$ (m is an integer). In fact:

$$\chi_G(x) = (A_G/a) \sum_{\Gamma} \hat{f}(G + \Gamma) \exp(i(G + \Gamma)x), \quad (9)$$

where $\hat{f}(q)$ is the Fourier transform of $f_0(x)$:

$$\hat{f}(q) = \int_{-\infty}^{\infty} dx f_0(x) e^{iqx}. \quad (10)$$

At this point, it is useful to note that for some choices of $f_0(x)$ the blip-function basis set is exactly equivalent to a plane-wave basis set. For this to happen, $\hat{f}(q)$ must be exactly zero beyond some cut-off wavevector q_{cut} . Then provided $q_{\text{cut}} \geq G_{\max}$ and provided $q_{\text{cut}} + G_{\max} < 2\pi/a$, all the $\Gamma \neq 0$ terms in Eq. (9) will vanish and all blip waves for $-G_{\max} \leq G \leq G_{\max}$ will be identical to plane-waves. (Of course, we must also require that $\hat{f}(q) \neq 0$ for $|q| \leq G_{\max}$.)

Our main aim in this Section is to determine how the total energy converges to the exact value as the width and spacing of the blip functions are varied. The spacing is controlled by varying a , and the width is controlled by scaling each blip function: $f_0(x) \rightarrow f_0(sx)$, where s is a scaling factor. In the case of blip functions for which $\hat{f}(q)$ cuts off in the way just described, the convergence of the total energy is easy to describe. Suppose we take a fixed blip width, and hence a fixed wavevector cut-off q_{cut} . If the blip spacing a is small enough so that $q_{\text{cut}} < \pi/a$, then it follows from what we have said that the blip basis set is exactly equivalent to a plane-wave basis set having $G_{\max} = q_{\text{cut}}$. This means that the total energy is equal to $E(q_{\text{cut}})$ and is completely independent of a when the latter falls below the threshold value $a_{\text{th}} = \pi/q_{\text{cut}}$. This is connected with the fact that the blip basis set becomes over-complete when $a < a_{\text{th}}$: there are linear dependences between the M blip functions $f_\ell(x)$.

It follows from this that the behavior of the total energy as a function of blip spacing and blip width is as shown schematically in Fig. 1. As the width is reduced,

the cut-off q_{cut} increases in proportion to the scaling factor s , so that the threshold spacing a_{th} is proportional to the width. The energy value $E(q_{\text{cut}})$ obtained for $a < a_{\text{th}}$ decreases monotonically with the width, as follows from the monotonic decrease of $E(G_{\text{max}})$ with G_{max} for a plane-wave basis set. Note that in Fig. 1 we have shown E at fixed width as decreasing monotonically with a for $a > a_{\text{th}}$. In fact, this may not always happen. Decrease of a does not correspond simply to addition of basis functions and hence to increase of variational freedom: it also involves relocation of the basis functions. However, what is true is that E for $a > a_{\text{th}}$ is always greater than E for $a < a_{\text{th}}$, as can be proved from the over-completeness of the blip basis set for $a < a_{\text{th}}$. At large spacings, the large-width blip basis is expected to give the lower energy, since in this region the poorer representation of long waves should be the dominant source of error.

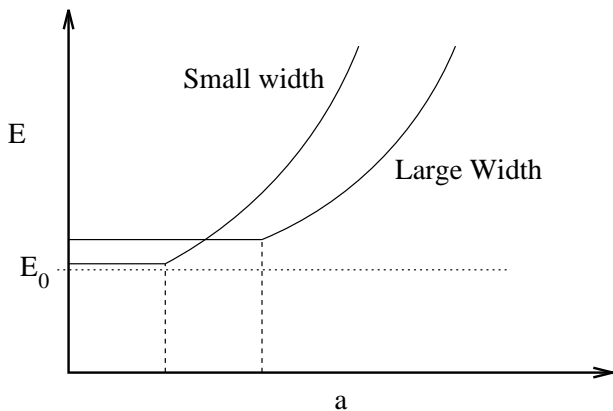


FIG. 1. Expected schematic form for the total ground-state energy as a function of the blip-grid spacing for two different blip widths, in the case where the Fourier components of the blip functions vanish beyond some cut-off. The horizontal dotted line shows the exact ground-state energy E_0 . The vertical dashed lines mark the threshold values a of blip grid spacing (see text).

Up to now, we have considered only the rather artificial case where the Fourier components of the blip function are strictly zero beyond a cut-off. This means that the blip function must extend to infinity in real space, and this is clearly no use if we wish to do all calculations in real space. We actually want $f_0(x)$ to be strictly zero beyond some real-space cut-off b_0 : $f_0(x) = 0$ if $|x| > b_0$. This means that $\hat{f}(q)$ will extend to infinity in reciprocal space. However, we can expect that with a judicious choice for the form of $f_0(x)$ the Fourier components $\hat{f}(q)$ will still fall off very rapidly, so that the behavior of the total energy is still essentially as shown in Fig. 1. If the choice is not judicious, we shall need a considerably greater effort to bring E within a specified tolerance of the exact value than if we were using a plane-wave basis set. With a plane-wave basis, a certain cut-off G_{max} is needed in order to achieve a specified tolerance in E .

With blip functions whose Fourier components cut off at G_{max} , we should need a blip spacing of π/G_{max} to achieve the same tolerance. Our requirement on the actual choice of blip function is that the spacing needed to achieve the given tolerance should be not much less than π/G_{max} .

B. B-splines as blip functions

Given that the blip function cuts off in real space at some distance b_0 , it is helpful if the function and some of its derivatives go smoothly to zero at this distance. If $f_0(x)$ and all its derivatives up to and including the n th vanish at $|x| = b_0$, then $\hat{f}(q)$ falls off asymptotically as $1/|q|^{n+2}$ as $|q| \rightarrow \infty$. One way of making a given set of derivatives vanish is to build $f_0(x)$ piecewise out of suitable polynomials. As an example, we examine here the choice of $f_0(x)$ as a B-spline.

B-splines are localized polynomial basis functions that are equivalent to a representation of functions in terms of cubic splines. A single B-spline $B(x)$ centered at the origin and covering the region $|x| \leq 2$ is built out of third-degree polynomials in the four intervals $-2 \leq x \leq -1$, $-1 \leq x \leq 0$, $0 \leq x \leq 1$ and $1 \leq x \leq 2$, and is defined as:

$$B(x) = \begin{cases} 1 - \frac{3}{2}x^2 + \frac{3}{4}|x|^3 & \text{if } 0 < |x| < 1 \\ \frac{1}{4}(2 - |x|)^3 & \text{if } 1 < |x| < 2 \\ 0 & \text{if } 2 < |x| \end{cases} \quad (11)$$

The function and its first two derivatives are continuous everywhere. The Fourier transform of $B(x)$, defined as in Eq. (10), is:

$$\hat{B}(q) = \frac{1}{q^4}(3 - 4 \cos q + \cos 2q), \quad (12)$$

which falls off asymptotically as q^4 , as expected. Our choice of blip function is thus $f_0(x) = B(2x/b_0)$, so that $\hat{f}(q) = \hat{B}(\frac{1}{2}b_0q)$.

The transform $\hat{B}(q)$ falls rapidly to small values in the region $|q| \simeq \pi$. It is exactly zero at the set of wavevectors $q_n = 2\pi n$ (n is a non-zero integer), and is very small in a rather broad region around each q_n , because the lowest non-vanishing term in a polynomial expansion of $3 - 4 \cos q + \cos 2q$ is of degree q^4 . This suggests that this choice of blip function will behave rather similarly to one having a Fourier cut-off $q_{\text{cut}} = 2\pi/b_0$. In other words, if we keep b_0 fixed and reduce the blip spacing a , the energy should approach the value obtained in a plane-wave calculation having $G_{\text{max}} = q_{\text{cut}}$ when $a \simeq \frac{1}{2}b_0$. The practical tests that now follow will confirm this. (We note that B-splines are usually employed with a blip spacing equal to $\frac{1}{2}b_0$; here, however, we are allowing the spacing to vary).

C. Practical tests

Up to now, it was convenient to work in one dimension, but for practical tests we clearly want to go to real three-dimensional systems. To do this, we simply take the blip function $f_0(\mathbf{r})$ to be the product of factors depending on the three Cartesian components of \mathbf{r} :

$$f_0(\mathbf{r}) = p_0(x)p_0(y)p_0(z). \quad (13)$$

All the considerations outlined above for a blip basis in one dimension apply unchanged to the individual factors $p_0(x)$ etc, which are taken here to be B-splines. Corresponding to the blip grid of spacing a in one dimension, the blip functions $f_0(\mathbf{r})$ now sit on the points of a three-dimensional grid which we assume here to be simple cubic. The statements made above about the properties of the B-spline basis are expected to remain true in this three-dimensional form.

We present here some tests on the performance of a B-spline basis for crystalline Si. At first sight, it might appear necessary to write a new code in order to perform such tests. However, it turns out that rather minor modifications to an existing plane-wave code allow one to produce results that are identical to those that would be obtained with a B-spline basis. For the purpose of the present tests, this is sufficient. The notion behind this device is that blip functions can be expanded in terms of plane waves, so that the function-space spanned by a blip basis is contained within the space spanned by a plane-wave basis, provided the latter has a large enough G_{\max} . Then all we have to do to get the blip basis is to project from the large plane-wave space into the blip space. Mathematical details of how to do this projection in practice are given in the Appendix. The practical tests have been done with the CASTEP code⁵, which we have modified to perform the necessary projections.

Our tests have been done on the diamond-structure Si crystal, using the Appelbaum-Hamann⁴⁰ local pseudopotential; this is an empirical pseudopotential, but suffices to illustrate the points of principle at issue here. The choice of k -point sampling is not expected to make much difference to the performance of blip functions, and we have done the calculations with a k -point set corresponding to the lowest-order 4 k -point Monkhorst-Pack⁴¹ sampling for an 8-atom cubic cell. If we go the next-order set of 32 k -points, the total energy per atom changes by less than 0.1 eV. For reference purposes, we have first used CASTEP in its normal unmodified plane-wave form to examine the convergence of total energy with respect to plane-wave cut-off for the Appelbaum-Hamann potential. We find that for plane-wave cut-off energies $E_{\text{pw}} = \hbar^2 G_{\max}^2 / 2m$ equal to 150, 250 and 350 eV, the total energies per atom are -115.52, -115.64 and -115.65 eV. This means that to obtain an accuracy of 0.1 eV/atom, a cut-off of 150 eV (corresponding to $G_{\max} = 6.31 \text{ \AA}^{-1}$) is adequate. According to the discussion of Sec. 2.2, the properties of this plane-wave basis

should be quite well reproduced by a blip-function basis of B-splines having half-width $b_0 = 2\pi/G_{\max} = 1.0 \text{ \AA}$, and the total energy calculated with this basis should converge rapidly to the plane-wave result when the blip spacing falls below $a \simeq \frac{1}{2}b_0 = 0.5 \text{ \AA}$.

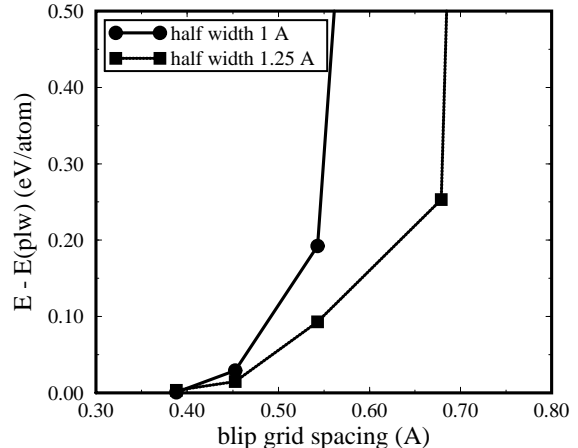


FIG. 2. Convergence of the total energy for two different blip half-widths as a function of the blip grid spacing. The calculations were performed with the Appelbaum-Hamann pseudopotential. $E(\text{plw})$ is the plane-wave result, obtained with a cutoff of 250 eV.

We have done the tests with two widths of B-splines: $b_0 = 1.25$ and 1.0 \AA , and in each case we have calculated E as a function of the blip spacing a . In all cases, we have used a plane-wave cut-off large enough to ensure that errors in representing the blip-function basis are negligible compared with the errors attributable to the basis itself. Our results for E as a function of a (Fig. 2) fully confirm our expectations. First, they have the general form indicated in Fig. 1. The difference is that since we have no sharp cut-off in reciprocal space, E does not become constant when a falls below a threshold, but instead continues to decrease towards the exact value. Second, for $b_0 = 1.0 \text{ \AA}$, E does indeed converge rapidly to the plane-wave result when a falls below $\sim 0.5 \text{ \AA}$. Third, the larger blip width gives the lower energy at larger spacings.

III. THE BLIP-FUNCTION BASIS IN LINEAR-SCALING CALCULATIONS

A. Technical matters

In our linear-scaling scheme, the support functions $\phi_\alpha(\mathbf{r})$ must be varied within support regions, which are centered on the atoms. These regions, taken to be spherical with radius R_{reg} in our previous work, move with the atoms. In the present work, the ϕ_α are represented

in terms of blip functions. Each atom has a blip grid attached to it, and this grid moves rigidly with the atom. The blip functions sit on the point of this moving grid. To make the region localized, the set of blip-grid points is restricted to those for which the associated blip function is wholly contained within the region radius R_{reg} . If we denote by $f_{\alpha\ell}(\mathbf{r})$ the ℓ th blip function in the region supporting ϕ_α , then the representation is:

$$\phi_\alpha(\mathbf{r}) = \sum_{\ell} b_{\alpha\ell} f_{\alpha\ell}(\mathbf{r}), \quad (14)$$

and the blip coefficients $b_{\alpha\ell}$ have to be varied to minimize the total energy.

The ϕ_α enter the calculation through their overlap matrix elements and the matrix elements of kinetic and potential energies. The overlap matrix $S_{\alpha\beta}$ [see Eq. (6)] can be expressed analytically in terms of the blip coefficients:

$$S_{\alpha\beta} = \sum_{\ell\ell'} b_{\alpha\ell} b_{\beta\ell'} s_{\alpha\ell,\beta\ell'}, \quad (15)$$

where $s_{\alpha\ell,\beta\ell'}$ is the overlap matrix between blip functions:

$$s_{\alpha\ell,\beta\ell'} = \int d\mathbf{r} f_{\alpha\ell} f_{\beta\ell'}, \quad (16)$$

which is known analytically. Similarly, the kinetic energy matrix elements:

$$T_{\alpha\beta} = -\frac{\hbar^2}{2m} \int d\mathbf{r} \phi_\alpha \nabla^2 \phi_\beta \quad (17)$$

can be calculated analytically by writing:

$$T_{\alpha\beta} = \sum_{\ell\ell'} b_{\alpha\ell} b_{\beta\ell'} t_{\alpha\ell,\beta\ell'}, \quad (18)$$

where:

$$t_{\alpha\ell,\beta\ell'} = -\frac{\hbar^2}{2m} \int d\mathbf{r} f_{\alpha\ell} \nabla^2 f_{\beta\ell'}. \quad (19)$$

However, matrix elements of the potential energy cannot be treated analytically, and their integrations must be approximated by summation on a grid. This ‘integration grid’ is, of course, completely distinct from the blip grids. It does not move with the atoms, but is a single grid fixed in space. If the position of the m th point on the integration grid is called \mathbf{r}_m , then the matrix elements of the local potential (pseudopotential plus Hartree and exchange-correlation potentials) are approximated by:

$$V_{\alpha\beta} = \int d\mathbf{r} \phi_\alpha V \phi_\beta \simeq \delta\omega_{\text{int}} \sum_m \phi_\alpha(\mathbf{r}_m) V(\mathbf{r}_m) \phi_\beta(\mathbf{r}_m), \quad (20)$$

where $\delta\omega_{\text{int}}$ is the volume per grid point. For a non-local pseudopotential, we assume the real-space version of the

Kleinman-Bylander⁴² representation, and the terms in this are also calculated as a sum over points of the integration grid. We note that the approximate equivalence of the B-spline and plane-wave bases discussed above gives us an expectation for the required integration-grid spacing h . In a plane-wave calculation, h should in principle be less than $\pi(2G_{\text{max}})$. But the blip-grid spacing is approximately $a = \pi G_{\text{max}}$. We therefore expect to need $h \approx \frac{1}{2}a$.

In order to calculate $V_{\alpha\beta}$ like this, we have to know all the values $\phi_\alpha(\mathbf{r}_m)$ on the integration grid:

$$\phi_\alpha(\mathbf{r}_m) = \sum_{\ell} b_{\alpha\ell} f_{\alpha\ell}(\mathbf{r}_m). \quad (21)$$

At first sight, it would seem that each point \mathbf{r}_m would be within range of a large number of blip functions, so that many terms would have to be summed over for each \mathbf{r}_m in Eq. (21). In fact, this is not so, provided the blip functions factorize into Cartesian components in the way shown in Eq. (13). To see this, assume that the blip grid and integration grid are cubic, let the blip-grid index ℓ correspond to the triplet (ℓ_x, ℓ_y, ℓ_z) , and let the factorization of $f_\ell(\mathbf{r})$ be written as:

$$f_\ell(\mathbf{r}_m) = p_{\ell_x}(x_m) p_{\ell_y}(y_m) p_{\ell_z}(z_m), \quad (22)$$

where x_m , y_m and z_m are the Cartesian components of \mathbf{r}_m (we suppress the index α for brevity). The sum over ℓ in Eq. (21) can then be performed as a sequence of three summations, the first of which is:

$$\theta_{\ell_y\ell_z}(x_m) = \sum_{\ell_x} b_{\ell_x\ell_y\ell_z} p_{\ell_x}(x_m). \quad (23)$$

The number of operations needed to calculate all these quantities $\theta_{\ell_y\ell_z}(x_m)$ is just the number of points (ℓ_x, ℓ_y, ℓ_z) on the blip grid times the number ν_{int} of points x_m for which $p_{\ell_x}(x_m)$ is non-zero for a given ℓ_x . This number ν_{int} will generally be rather moderate, but the crucial point is that the number of operations involved is proportional only to ν_{int} and not to ν_{int}^3 . Similar considerations will apply to the sums over ℓ_y and ℓ_z .

It is worth remarking that since we have to calculate $\phi_\alpha(\mathbf{r}_m)$ anyway, we have the option of calculating $S_{\alpha\beta}$ by direct summation on the grid as well. In fact, $T_{\alpha\beta}$ can also be treated this way, though here one must be more careful, since it is essential that its symmetry ($T_{\alpha\beta} = T_{\beta\alpha}$) be preserved by whatever scheme we use. This can be achieved by, for example, calculating the gradient $\nabla\phi_\alpha(\mathbf{r}_m)$ analytically on the integration grid and then using integration by parts to express $T_{\alpha\beta}$ as an integral over $\nabla\phi_\alpha \cdot \nabla\phi_\beta$. In the present work, we use the analytic forms for $s_{\alpha\ell,\beta\ell'}$ and $t_{\alpha\ell,\beta\ell'}$.

A full linear-scaling calculation requires minimization of the total energy with respect to the quantities ϕ_α and $L_{\alpha\beta}$. However, at present we are concerned solely with the representation of ϕ_α , and the cut-off applied to $L_{\alpha\beta}$ is irrelevant. For our practical tests of the blip-function

basis, we have therefore taken the $L_{\alpha\beta}$ cut-off to infinity, which is equivalent to exact diagonalization of the Kohn-Sham equation. Apart from this, the procedure we use for determining the ground state, i.e. minimizing E with respect to the ϕ_α functions, is essentially the same as in our previous work^{22,23}. We use conjugate-gradients⁴³ minimization with respect to the blip-function coefficients $b_{\alpha\ell}$. Expressions for the required derivatives are straightforward to derive using the methods outlined earlier²³.

B. Practical tests

We present here numerical tests both for the Appelbaum-Hamann⁴⁰ local pseudopotential for Si used in Sec. 2 and for a standard Kerker⁴⁴ non-local pseudopotential for Si. The aims of the tests are: first, to show that the B-spline basis gives the accuracy in support-function calculations to be expected from our plane-wave calculations; and second to examine the convergence of E towards the exact plane-wave results as the region radius R_{reg} is increased. For present purposes, it is not particularly relevant to perform the tests on large systems. The tests have been done on perfect-crystal Si at the equilibrium lattice parameter, as in Sec. 2.3.

h (Å)	E (eV/atom)
0.4525	-0.25565
0.3394	0.04880
0.2715	0.00818
0.2263	-0.01485
0.1940	0.00002
0.1697	-0.00270
0.1508	0.00000

TABLE I. Total energy E as a function of integration grid spacing h using a region radius $R_{\text{reg}} = 2.715$ Å. The blip half-width b_0 was set to 0.905 Å and the blip grid spacing used was 0.4525 Å. The zero of energy is set equal to the result obtained with the finest grid.

We have shown in Sec. 2.3 that a basis of B-splines having a half-width $b_0 = 1.0$ Å gives an error of ~ 0.1 eV/atom if the blip spacing is ~ 0.45 Å. For the present tests we have used the similar values $b_0 = 0.905$ Å and $a = 0.4525$ Å, in the expectation of getting this level of agreement with CASTEP plane-wave calculations in the limit $R_{\text{reg}} \rightarrow \infty$. To check the influence of integration grid spacing h , we have made a set of calculations at different h using $R_{\text{reg}} = 2.715$ Å, which is large enough to be representative (see below). The results (Table 1) show that E converges rapidly with decreasing h , and ceases to vary for present purposes when $h = 0.194$ Å. This confirms our expectation that $h \approx \frac{1}{2}a$. We have then used this grid spacing to study the variation of E with R_{reg} , the results for which are given in Table 2, where we also compare with the plane-wave results. The extremely rapid convergence of E when R_{reg} exceeds ~ 3.2 Å is very striking, and our results show that R_{reg} values yielding an accuracy of 10^{-3} eV/atom are easily attainable. The close agreement with the plane-wave result fully confirms the effectiveness of the blip-function basis. As expected from the variational principle, E from the blip-function calculations in the $R_{\text{reg}} \rightarrow \infty$ limit lies slightly above the plane-wave value, and the discrepancy of ~ 0.1 eV is of the size expected from the tests of Sec. 2.3 for (nearly) the present blip-function width and spacing. (We also remark in parenthesis that the absolute agreement between results obtained with two entirely different codes is useful evidence for the technical correctness of our codes.)

R_{reg} (Å)	E (eV/atom)	
	local pseudopotential	non-local pseudopotential
2.2625	1.8659	1.9653
2.7150	0.1554	0.1507
3.1675	0.0559	0.0396
3.6200	0.0558	0.0396
4.0725	0.0558	0.0396

TABLE II. Convergence of the total energy E as a function of the region radius R_{reg} for silicon with a local and a non-local pseudopotential. The calculations were performed with a blip grid spacing of 0.4525 Å and a blip half-width of 0.905 Å in both cases. The zero of energy was taken to be the plane wave result obtained with each pseudopotential, with plane wave cutoffs of 250 and 200 eV respectively.

The results obtained in our very similar tests using the Kleinman-Bylander form of the Kerker pseudopotential for Si are also shown in Table 2. In plane-wave calculations, the plane-wave cut-off needed for the Kerker potential to obtain a given accuracy is very similar to that needed in the Appelbaum-Hamann potential, and we have therefore used the same B-spline parameters. Tests on the integration-grid spacing show that we can use the value $h = 0.226 \text{ \AA}$, which is close to what we have used with the local pseudopotential. The total energy converges in the same rapid manner for $R_{\text{reg}} > 3.2 \text{ \AA}$, and the agreement of the converged result with the CASTEP value is also similar to what we saw with the Appelbaum-Hamann pseudopotential.

IV. DISCUSSION

In exploring the question of basis sets for linear-scaling calculations, we have laid great stress on the relation with plane-wave basis sets. One reason for doing this is that the plane-wave technique is the canonical method for pseudopotential calculations, and provides the easiest way of generating definitive results by going to basis-set convergence. We have shown that within the linear-scaling approach the total energy can be taken to converge by systematically reducing the width and spacing of a blip-function basis set, just as it can be taken to convergence by increasing the plane-wave cut-off in the canonical method. By analyzing the relation between the plane-wave and blip-function bases, we have also given simple formulas for estimating the blip width and spacing needed to achieve the same accuracy as a given plane-wave cut-off. In addition, we have shown that the density of integration-grid points relates to the number of blip functions in the same way as it relates to the number of plane waves. Finally, we have seen that the blip-function basis provides a practical way of representing support functions in linear-scaling calculations, and that the total energy converges to the plane-wave result as the region radius is increased.

These results give useful insight into what can be expected of linear-scaling DFT calculations. For large systems, the plane-wave method requires a massive redundancy of information: it describes the space of occupied states using a number of variables of order $N \times M$ (N the number of occupied orbitals, M the number of plane waves), whereas the number of variables in a linear-scaling method is only of order $N \times m$ (m the number of basis functions for each support function). This means that the linear-scaling method needs fewer variables than the plane-wave method by a factor m/M . But we have demonstrated that to achieve a given accuracy the number of blip functions per unit volume is not much greater than the number of plane waves per unit volume. Then the factor m/M is roughly the ratio between the volume of a support region and the volume of the entire sys-

tem. The support volume must clearly depend on the nature of the system. But for the Si system, we have seen that convergence is extremely rapid once the region radius exceeds $\sim 3.2 \text{ \AA}$, corresponding to a region volume of 137 \AA^3 , which is about 7 times greater than the volume per atom of 20 \AA^3 . In this example, then, the plane-wave method needs more variables than the linear-scaling method when the number of atoms N_{atom} is greater than ~ 7 , and for larger systems it needs more variables by a ‘redundancy factor’ of $\sim N_{\text{atom}}/7$. (For a system of 700 atoms, e.g., the plane-wave redundancy factor would be ~ 100 .) In this sense, plane-wave calculations on large systems are grossly inefficient. However, one should be aware that there are other factors in the situation, like the number of iterations needed to reach the ground state in the two methods. We are not yet in a position to say anything useful about this, but we plan to return to it.

Finally, we note an interesting question. The impressive rate of convergence of ground-state energy with increase of region radius shown in Table 2 raises the question of what governs this convergence rate, and whether it will be found in other systems, including metals. We remark that this is not the same as the well-known question about the rate of decay of the density matrix $\rho(\mathbf{r}, \mathbf{r}')$ as $|\mathbf{r} - \mathbf{r}'| \rightarrow \infty$, because in our formulation both $\phi_\alpha(\mathbf{r})$ and $L_{\alpha\beta}$ play a role in the decay. Our intuition is that this decay is controlled by $L_{\alpha\beta}$. We hope soon to report results on the support functions for different materials, which will shed light on this.

ACKNOWLEDGEMENTS

This project was performed in the framework of the U.K. Car-Parrinello Consortium, and the work of CMG is funded by the High Performance Computing Initiative (HPCI) through grant GR/K41649. The work of EH is supported by EPSRC grant GR/J01967. The use of B-splines in the work arose from discussions with James Annett.

APPENDIX: USING PLANE-WAVE CALCULATIONS TO TEST BLIP FUNCTIONS

We explain here in more detail how a standard plane-wave code can be used to test the performance of blip-function basis sets (see Sec. 2.3).

In a plane-wave calculation, the occupied orbitals $\psi_i(\mathbf{r})$ are expressed as:

$$\psi_i(\mathbf{r}) = \Omega^{-1/2} \sum_{\mathbf{G}} c_{i\mathbf{G}} \exp(i\mathbf{G} \cdot \mathbf{r}), \quad (\text{A1})$$

where \mathbf{G} goes over all reciprocal lattice vectors whose magnitude is less than the plane-wave cut-off G_{max} , and Ω is the volume per cell. (We assume Γ -point sampling

for simplicity.) The usual procedure is to minimize the total energy E with respect to the plane-wave coefficients $c_{i\mathbf{G}}$, subject to the orthonormality constraints:

$$\sum_{\mathbf{G}} c_{i\mathbf{G}}^* c_{j\mathbf{G}} = \delta_{ij} . \quad (\text{A2})$$

In a blip-function basis, the orbitals can be regarded as expanded in terms of the blip waves $\chi_{\mathbf{G}}(\mathbf{r})$ defined by:

$$\chi_{\mathbf{G}}(\mathbf{r}) = A_{\mathbf{G}} \sum_{\ell} f_{\ell}(\mathbf{r}) \exp(i\mathbf{G} \cdot \mathbf{R}_{\ell}) , \quad (\text{A3})$$

where the sum goes over all blip-grid points in one repeating cell, and \mathbf{G} is any of the reciprocal-lattice vectors of the repeating cell in the Brillouin zone associated with the blip grid. (The number of different \mathbf{G} vectors labelling $\chi_{\mathbf{G}}$ is thus the same as the number of points of the blip grid in one cell.) The $\chi_{\mathbf{G}}(\mathbf{r})$ are orthogonal for different values of \mathbf{G} , and we assume that the constant $A_{\mathbf{G}}$ is chosen so that the $\chi_{\mathbf{G}}(\mathbf{r})$ are normalized:

$$\int d\mathbf{r} \chi_{\mathbf{G}_1}^* \chi_{\mathbf{G}_2} = \delta_{\mathbf{G}_1, \mathbf{G}_2} . \quad (\text{A4})$$

Then the orbitals are represented in terms of the blip waves as:

$$\psi_i(\mathbf{r}) = \sum_{\mathbf{G}} b_{i\mathbf{G}} \chi_{\mathbf{G}}(\mathbf{r}) , \quad (\text{A5})$$

and the ground state is determined by minimizing E with respect to the blip coefficients $b_{i\mathbf{G}}$ subject to orthonormality:

$$\sum_{\mathbf{G}} b_{i\mathbf{G}}^* b_{j\mathbf{G}} = \delta_{ij} . \quad (\text{A6})$$

Now the $c_{i\mathbf{G}}$ can be expressed in terms of the $b_{i\mathbf{G}}$ by using the expansion of $\chi_{\mathbf{G}}(\mathbf{r})$ in terms of plane waves:

$$\chi_{\mathbf{G}}(\mathbf{r}) = A_{\mathbf{G}} \omega^{-1} \sum_{\mathbf{\Gamma}} \hat{f}(\mathbf{G} + \mathbf{\Gamma}) \exp [i(\mathbf{G} + \mathbf{\Gamma}) \cdot \mathbf{r}] , \quad (\text{A7})$$

where $\hat{f}(\mathbf{q})$ is the Fourier transform of $f_0(\mathbf{r})$, ω is the volume per blip-grid point, and $\mathbf{\Gamma}$ goes over the reciprocal-lattice vectors of the blip grid. From this, we have:

$$\psi_i(\mathbf{r}) = \omega^{-1} \sum_{\mathbf{G}} A_{\mathbf{G}} b_{i\mathbf{G}} \sum_{\mathbf{\Gamma}} \hat{f}(\mathbf{G} + \mathbf{\Gamma}) \exp [i(\mathbf{G} + \mathbf{\Gamma}) \cdot \mathbf{r}] , \quad (\text{A8})$$

so that:

$$c_{i\mathbf{G}+\mathbf{\Gamma}} = \Omega^{1/2} \omega^{-1} A_{\mathbf{G}} b_{i\mathbf{G}} \hat{f}(\mathbf{G} + \mathbf{\Gamma}) . \quad (\text{A9})$$

Note that in interpreting this equation, \mathbf{G} must be taken in the first Brillouin zone of the blip grid.

This equation implies a relation between the plane-wave coefficients $c_{i\mathbf{G}+\mathbf{\Gamma}}$ for the same values of \mathbf{G} but

different $\mathbf{\Gamma}$. We can therefore reproduce the effect of a blip-function basis set by performing a standard plane-wave calculation in which the $c_{i\mathbf{G}+\mathbf{\Gamma}}$ are constrained to obey this relation. Note that in practice the plane-wave calculation must involve a plane-wave cut-off, so that the $c_{i\mathbf{G}+\mathbf{\Gamma}}$ will actually be set to zero when $|\mathbf{G} + \mathbf{\Gamma}|$ exceeds this cut-off. This is equivalent to setting $\hat{f}(\mathbf{G} + \mathbf{\Gamma})$ equal to zero beyond the cut-off, and this amounts to a small smoothing of the blip function in real space. Allowing for this modification, the space spanned by the blip functions is a sub-space of the space spanned by the plane waves. The constraint on the $c_{i\mathbf{G}+\mathbf{\Gamma}}$ is therefore a linear relation between these coefficients which expresses the fact that their component orthogonal to the sub-space vanishes. It can be written as:

$$0 = c_{i\mathbf{G}+\mathbf{\Gamma}} - \hat{f}(\mathbf{G} + \mathbf{\Gamma}) \sum_{\mathbf{\Gamma}'} \hat{f}^*(\mathbf{G} + \mathbf{\Gamma}') c_{i\mathbf{G}+\mathbf{\Gamma}'} / \sum_{\mathbf{\Gamma}'} |\hat{f}(\mathbf{G} + \mathbf{\Gamma}')|^2 . \quad (\text{A10})$$

The modifications to the plane-wave code are therefore very simple. First, the initial guess for the orbitals must be chosen so as to satisfy this condition. Second, when the $c_{i\mathbf{G}+\mathbf{\Gamma}}$ are updated on the iterative path to the self-consistent ground state, the changes of $c_{i\mathbf{G}+\mathbf{\Gamma}}$ must be projected so as to satisfy this condition. This means that if the unconstrained calculation would have produced the changes $\delta c_{i\mathbf{G}+\mathbf{\Gamma}}$, these must be replaced by $\delta c_{i\mathbf{G}+\mathbf{\Gamma}}^{\parallel}$ given by:

$$\delta c_{i\mathbf{G}+\mathbf{\Gamma}}^{\parallel} = \hat{f}(\mathbf{G} + \mathbf{\Gamma}) \sum_{\mathbf{\Gamma}'} \hat{f}^*(\mathbf{G} + \mathbf{\Gamma}') \delta c_{i\mathbf{G}+\mathbf{\Gamma}'} / \sum_{\mathbf{\Gamma}'} |\hat{f}(\mathbf{G} + \mathbf{\Gamma}')|^2 . \quad (\text{A11})$$

This will produce exactly the same result as if we had worked directly with blip functions.

¹ P. Hohenberg and W. Kohn, Phys. Rev., **136**, B864 (1964).

² W. Kohn and L.J. Sham, Phys. Rev., **140**, A1133 (1965).

³ M.J. Gillan, in *Computer Simulation in Materials Science*, edited by M. Meyer and V. Pontikis, Kluwer, Dordrecht (1991).

⁴ G. Galli and A. Pasquarello, in *Computer Simulation in Chemical Physics*, edited by M.P. Allen and D.J. Tildesley, Kluwer, Dordrecht (1993).

⁵ M.C. Payne, M.P. Teter, D.C. Allan, T.A. Arias and J.D. Joannopoulos, Rev. Mod. Phys. **64**, 1045 (1993).

⁶ R. Car and M. Parrinello, Phys. Rev. Lett. **55**, 2471 (1985).

⁷ W. Yang, Phys. Rev. Lett. **66**, 1438 (1991).

⁸ W. Yang, J. Mol. Str. (Theochem) **255**, 461 (1992).

⁹ C. Lee and W. Yang, J. Chem. Phys. **96**, 2408 (1992).

- ¹⁰ J.-P. Lu and W. Yang, Phys. Rev. B **49**, 11421 (1994).
- ¹¹ W. Yang and T.S. Lee, J. Chem. Phys. **103**, 5674 (1995).
- ¹² S. Baroni and P. Giannozzi, Europhys. Lett. **17**, 547 (1992).
- ¹³ G. Galli and M. Parrinello, Phys. Rev. Lett. **69**, 3547 (1992).
- ¹⁴ F. Mauri, G. Galli and R. Car, Phys. Rev. B **47**, 9973 (1993).
- ¹⁵ F. Mauri and G. Galli, Phys. Rev. B **50**, 4316 (1994).
- ¹⁶ J. Kim, F. Mauri and G. Galli, Phys. Rev. B, **52**, 1640 (1995).
- ¹⁷ P. Ordejón, D.A. Drabold, M.P. Grumbach and R.M. Martin, Phys. Rev. B **48**, 14646 (1993).
- ¹⁸ P. Ordejón, D.A. Drabold, R.M. Martin, and M.P. Grumbach, Phys. Rev. B **51**, 1456 (1995).
- ¹⁹ X.P. Li, R.W. Nunes and D. Vanderbilt, Phys. Rev. B **47**, 10891 (1993).
- ²⁰ R.W. Nunes and D. Vanderbilt, Phys. Rev. B **50**, 17611 (1994).
- ²¹ W. Hierse and E.B. Stechel, Phys. Rev. B **50**, 17811 (1994).
- ²² E. Hernández and M.J. Gillan, Phys. Rev. B **51**, 10157 (1995).
- ²³ E. Hernández, M.J. Gillan and C.M. Goringe, Phys. Rev. B **53**, 7147 (1996).
- ²⁴ P. Ordejón, E. Artacho and J.M. Soler, Phys. Rev. B, **53**, 10441 (1996).
- ²⁵ J.R. Chelikowsky, N. Troullier and Y. Saad, Phys. Rev. Lett. **72**, 1240 (1994).
- ²⁶ X. Jing, N. Troullier, D. Dean, N. Binggeli, J.R. Chelikowsky, K. Wu and Y. Saad, Phys. Rev. B **50**, 12234 (1994).
- ²⁷ J.R. Chelikowsky, N. Troullier, K. Wu and Y. Saad, Phys. Rev. B **50**, 11355 (1994).
- ²⁸ F. Gygi, Europhys. Lett. **19**, 617 (1992).
- ²⁹ F. Gygi, Phys. Rev. B **48**, 11692 (1993).
- ³⁰ F. Gygi, Phys. Rev. B **51**, 11190 (1995).
- ³¹ A.P. Seitsonen, M.J. Puska and R.M. Nieminen, Phys. Rev. B **51**, 14057 (1995).
- ³² D.R. Hamann, Phys. Rev. B, **51**, 7337 (1995).
- ³³ D.R. Hamann, Phys. Rev. B **51**, 9508 (1995).
- ³⁴ E.L. Briggs, D.J. Sullivan and J. Bernholc, Phys. Rev. B **52**, 5471 (1995).
- ³⁵ K. Cho, T.A. Arias, J.D. Joannopoulos and P.K. Lam, Phys. Rev. Lett. **71**, 1387 (1993).
- ³⁶ C.C. Chen, H.P. Chang and C.S. Hsue, Chem. Phys. Lett. **217**, 486 (1994).
- ³⁷ J.P. Modisette, P. Nordlander, J.L. Kinsley and B.R. Johnson, Chem. Phys. Lett. **250**, 485 (1996).
- ³⁸ S.Q. Wei and M.Y. Chou, Phys. Rev. Lett. **76**, 2650 (1996).
- ³⁹ L.J. Clarke, I. Štich and M.C. Payne, Comp. Phys. Comm. **72**, 14 (1992).
- ⁴⁰ J.A. Appelbaum and D.R. Hamann, Phys. Rev. B **8**, 1777 (1973).
- ⁴¹ H.J. Monkhorst and J.D. Pack, Phys. Rev. B **13**, 5188 (1976).
- ⁴² L. Kleinman and D.M. Bylander, Phys. Rev. Lett. **48**, 1425 (1982).
- ⁴³ *Numerical Recipes: The Art of Scientific Computing* (2nd edition) by W.H. Press, S.A. Teukolsky, W.T. Vetterling and B.P. Flannery, Cambridge University Press, Cambridge (1992).
- ⁴⁴ G.P. Kerker, J. Phys. C, **13**, L189 (1980).